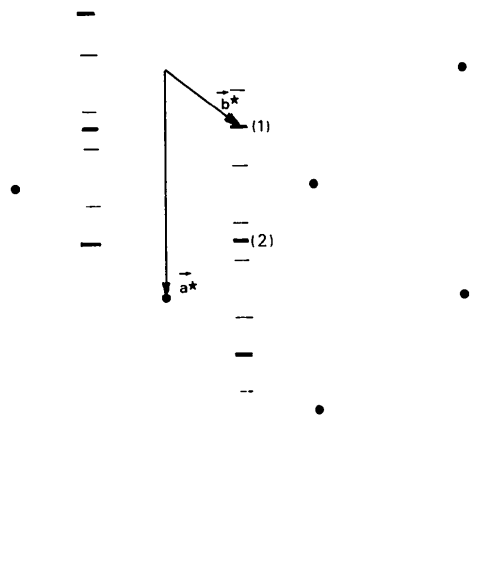

Fig. 9. Disposition relative des raies satellites et des réflexions de Bragg obtenues sur un cliché de précession *hk*0. Les réflexions (1) et leurs satellites proviennent de l'individu de plus grand volume dans l'édifice maclé, les réflexions (2) et leurs satellites de l'individu de plus petit volume. • réflexions intenses de symétrie monoclinique presque parfaite.

Les diagrammes de diffraction théoriques et observés *hk*0 sont comparés sur les Figs. 8 et 9. Dans les deux premiers cas, les réflexions de Bragg $k = 2n + 1$ sont éteintes et seules les raies satellites d'ordre impair sont allumées. Dans le troisième cas, les intensités des réflexions $k = 2n + 1$ ne sont pas nulles et il existe des raies satellites d'ordres pair et impair; $i = 0$ pour $k = 2n$ quelque soit le type de modulation.

Pour rendre compte de l'aspect des diagrammes (Fig. 2), qui comportent à la fois des réflexions de Bragg $k = 2n + 1$ et des raies satellites d'ordre impair, nous formulons l'hypothèse suivante: le cristal serait constitué de zones différentes, des zones D où interviendrait une modulation symétrique du type précédent et des zones D' sans modulation où Cd(3) et Ca réaliseraient de façon préférentielle la configuration planaire (1), la configuration (2) ayant une probabilité faible (cette supposition est compatible avec le fait que les réflexions $k = 2n + 1$ sont plus intenses pour $l = 2n + 1$ que pour $l = 2n$, Fig. 2). Soient N et N' le nombre de zones D et D' et I' l'intensité des réflexions de Bragg $k = 2n + 1$ issues des zones D'; en supposant que ces zones possèdent en moyenne le même volume, on trouve que le rapport $I'/i_{n=1} \simeq (N'/N)(M^2/4)\sin^2(\pi/M)$ est constant, en accord avec l'observation. A partir de la valeur mesurée de $I'/i_{n=1}$ qui est égale à 4,2 $\pm$0,1 (elle se rapporte à l'individu de plus grand volume dans l'édifice maclé), on déduit que la plus grande partie du cristal pourrait contenir environ deux fois plus de zones D' que de zones D. La relation qui apparaît entre $\lambda(2)$ et $\lambda(1)$ [$\lambda(2) \simeq 2\lambda(1)$] ne peut être expliquée à partir de ce modèle.

L'existence de domaines antiphase périodiques et de domaines maclés dans les cristaux de φ_5 s'accorde bien avec les conditions énoncées par Wondratschek & Jeitschko (1976): le groupe spatial $P\bar{1}$ de la structure 'dérivée' (φ_5) est un sous groupe général du groupe spatial ($C2/m$) de la structure 'parente' (Fig. 4*a*), qui correspond ici à une structure hypothétique.

Références

Bassett, H. & Strain, R. N. C. (1952). *J. Chem. Soc.* **2**, 1795–1806.

Böhm, H. (1975). *Acta Cryst.* A**31**, 622–628.

Britton, D. (1972). *Acta Cryst.* A**28**, 296–297.

Brown, I. D. & Shannon, R. D. (1973). *Acta Cryst.* A**29**, 266–282.

Cromer, D. T. (1965). *Acta Cryst.* **18**, 17–23.

Cromer, D. T. & Waber, J. T. (1965). *Acta Cryst.* **18**, 104–109.

Leligny, H. (1987). Thèse Doctorat Etat, UFR Sciences, Univ. de Caen.

Leligny, H. & Monier, J. C. (1978). *Acta Cryst.* B**34**, 3341–3343.

Leligny, H. & Monier, J. C. (1982). *Acta Cryst.* B**28**, 355–358.

Leligny, H. & Monier, J. C. (1983). *Acta Cryst.* C**39**, 947–952.

Leligny, H. & Monier, J. C. (1989). *Acta Cryst.* B**45**, 113–117.

Wondratschek, H. & Jeitschko, W. (1976). *Acta Cryst.* A**32**, 664–666.

Acta Cryst. (1989). B**45**, 124–128

Atomic Scale Mechanism of Ca*X* Zeolite Dehydration

By Yuri I. Smolin, Yuri F. Shepelev and Alexandra A. Anderson

Institute of Silicate Chemistry of the USSR, Academy of Sciences, 199034 *Leningrad, USSR*

(*Received* 26 *August* 1988; *accepted* 16 *November* 1988)

Abstract

The crystal structure of Ca-exchanged *X* zeolite [$Ca_{46}Al_{92}Si_{100}O_{384}.200H_2O$, cubic, $Fd3$, $a = 25{\cdot}06\ (1)$ Å, $Z = 1$, $F(000) = 8588$, $\lambda(\text{Mo } K\alpha) = 0{\cdot}71069$ Å, $\mu = 8{\cdot}1\ \text{cm}^{-1}$, $V = 15738\ (18)$ Å^3, $D_x = 1{\cdot}78\ \text{g cm}^{-3}$] has been determined by single-crystal X-ray diffraction at the following temperatures: 298 K

0108-7681/89/020124-05$03.00

Table 1. *Experimental and refinement details*

Temperature (K)	298	348	423	573	673	298 (rehydrated)
No. of unique reflections measured	739	330	424	460	279	392
No. of unique reflections observed $I > 3\sigma(I)$	589	263	343	350	220	310
$(\sin\theta/\lambda)_{max}$ (Å^{-1})	0·81	0·71	0·71	0·71	0·81	0·81
$(h,k,l)_{max}$	36,36,13	29,30,12	29,30,12	28,30,11	33,36,10	36,36,12
No. of parameters refined	100	80	78	76	78	86
R (%)	6·3	4·8	5·7	6·0	4·2	6·4
wR (%)	8·0	8·1	7·2	7·0	5·5	8·1
Low-order refinement, $\sin\theta/\lambda \le 0{\cdot}35$ Å^{-1}						
No. of unique reflections	143	100	114	129	134	109
No. of occupancy factors refined	8	6	5	5	4	7
R (%)	6·5	5·3	6·1	5·3	4·3	7·2
wR (%)	8·3	7·1	8·1	6·7	5·8	9·5

(589 unique observed reflections, $R = 6{\cdot}3\%$); 348 K (263, 4·8%); 423 K (343, 5·7%); 573 K (350, 6·0%); 673 K (220, 4·2%); and after rehydration in air at 298 K [$a = 25{\cdot}08$ (1) Å, 310 reflections, $R = 6{\cdot}4\%$]. In the crystal structure investigations a single crystal of regular octahedral shape with 0·2 mm edges was heated by a stream of hot N_2 gas. The investigations were focused on the migration of cations during dehydration of the crystal at increasing temperature. In the initial hydrated form calcium ions are located in sodalite cages and supercages. These ions are rather mobile and with removal of water from the crystal on heating they migrate in the direction of hexagonal prisms and sites on the six-membered ring faces of sodalite cages on the supercage side. After rehydration the initial distribution of Ca cations is restored.

Introduction

The structure of Ca-exchanged forms of faujasite-type zeolites with various Si/Al ratios have already been studied in hydrated and dehydrated states [Si/Al = 2·37, Bennet & Smith (1968*a*,*b*); Si/Al = 1·4, Pluth & Smith (1973*a*,*b*)]. These studies have shown that the Ca^{2+} ions are distributed over different sites within the zeolite framework and that the populations of these sites are markedly dependent on the presence of absorbed water molecules.

The present article is concerned with the study of the atomic scale mechanism of dehydration of Ca-exchanged *X* zeolite with an Si/Al ratio of 1·09 by determining the crystal structure at different temperatures.

Experimental

Crystals of Na*X* zeolite with Si/Al = 1·09 were grown by hydrothermal synthesis from aluminosilicate gels at 338 K using a modified version of Charnel's method (Bogomolov & Petranovsky, 1986). The crystals possessed a regular octahedral shape with 0·2 mm edges. These single crystals of Na*X* zeolite were used to prepare Ca*X* zeolite by ion exchange with a 0·35*M* aqueous solution of $Ca(NO_3)_2$ at room temperature. The exposure time was six months. Chemical analysis of the resulting product gave $Ca_{46}Al_{92}Si_{100}O_{384}\cdot 200H_2O$ per unit cell ($Ca_{46}X$). Six cycles of intensity measurements were carried out at various temperatures on a computer-controlled three-circle diffractometer with graphite-monochromated Mo $K\alpha$ radiation ($\lambda = 0{\cdot}71069$ Å). A perpendicular inclination technique was used. The *c* axis of the crystal was oriented along the ω axis of diffractometer. The cubic unit-cell parameter was determined from the 22,22,0 and 18,18,0 reflections. The crystal was heated by a stream of hot gas evaporated from liquid N_2. The temperature of the sample during a data collection cycle was stable within ± 1 K, the accuracy on an absolute scale was better than ± 3 K. The ω-step-scan mode (15 steps) was employed with a scan speed of 1·2° min^{-1} in ω and fixed counter aperture, $\Delta 2\theta = 1{\cdot}5°$; the background was determined using the algorithm of Oatley & French (1982). The reflection 12,12,0 was used as standard, its maximum intensity variation was 3%: the intensity data were corrected for this variation. The intensity data with $I \ge 3\sigma(I)$ were collected within the range $h \ge 0$, $k \ge 0$, $l \ge 0$ and $h \ge l$, $k \ge l$. All intensities were corrected for Lorentz and polarization effects, no absorption or extinction corrections were applied ($\mu = 8{\cdot}1$ cm^{-1}). Other experimental details are listed in Table 1. The last experiment (298 K, rehydrated) was carried out after exposure of the crystal to air for 3 days.

The structures of all six forms of $Ca_{46}X$ zeolite at various dehydration stages were analysed in space group *Fd*3. The origin of the coordinates was set on the centre of symmetry for convenience of computation. All calculations were performed with the *RENTGEN*75 package on a BESM-6 computer (Andrianov, Saphina & Tarnopolsky, 1974). Atomic scattering factors of neutral atoms (Hanson, Herman, Lea & Skillman, 1964) and Cruickshank's weighting scheme (Cruickshank, 1965) were used. Atomic coordinates from the Na*X* framework (Smolin, Shepelev, Butikova & Petranovsky, 1983) were utilized as initial parameters in the refinements of the Ca*X* forms. The refinement of layer scale factors, and positional and thermal parameters was carried out by blocked full-matrix least squares using all observed structure

factors. The non-framework Ca and O atoms were located from several difference Fourier syntheses. The final difference Fourier map showed no significant residual peaks. In order to avoid the correlation between thermal parameters and site-occupancy factors the occupancy factors of non-framework atoms were refined using low-order reflections with $\sin\theta/\lambda \leq 0{\cdot}35$ Å^{-1}. The framework atoms, Si, Al, O(1)–O(6), and some non-framework atoms with high occupancy factors were refined with anisotropic thermal parameters.

The final atomic coordinates, isotropic thermal parameters and occupancy factors are listed in Table 2.*

Discussion

Zeolite *X* is the synthetic counterpart of the naturally occurring mineral faujasite. An outline of the structure of faujasite-type zeolites is given in Fig. 1. The vertices of the polyhedra are occupied by the framework Si or Al atoms, which are in turn tetrahedrally bonded to the framework O atoms; these O atoms and the exchangeable cations are not shown for clarity. The polyhedron with 14 vertices is known as the sodalite or β-cage and is the principal building block of the framework. These β-cages are connected by double six-membered rings (hexagonal prisms), forming an interconnected set of even larger cavities accessed through 12-membered windows. The cations and water molecules are distributed in this zeolite type mainly over the sites I, I′, II′, II and III shown in Fig. 1. The nomenclature is as follows: site I, centre of hexagonal prism; site II, six-membered ring face of β-cage on the supercage side; sites I′ and II′ lie on the opposite sides of the six-membered rings as compared with sites I and II, respectively, and inside the β-cage; site III, at the edges of the four-membered rings inside the supercage.

Ca cations in the hydrated form are located in sites I′, II and III. The observed bond distances suggest the possibility of mixed occupancy on site III in the supercage (~9Ca + 19H_2O). In addition cations are present in site II′. In this position, with the multiplicity factor 32, an electron density maximum was revealed, the site-occupancy refinement of which gave an impossibly high content of H_2O molecules – *i.e.* 42·8. If one assumes that Ca scatters X-rays 2·5 times more strongly than H_2O, full occupancy of site II′ would be obtained by 7·2Ca and 24·8H_2O. In the hydrated form Ca cations are surrounded by O atoms of the aluminosilicate framework and water molecules. Inter-

Table 2. *Fractional coordinates, population parameters and equivalent isotropic temperature factors*

E.s.d.'s are given in parentheses. Origin at centre ($\bar{3}$) of space group *Fd*3.

	Population	Occupancy	*x*	*y*	*z*	B_{eq}(Å^2)
298 K						
Si	96	1	−0·0529 (1)	0·1254 (1)	0·0364 (1)	1·2
Al	96	1	−0·0534 (1)	0·0366 (1)	0·1247 (1)	1·1
O(1)	96	1	−0·1062 (3)	−0·0004 (3)	0·1044 (3)	3·1
O(2)	96	1	−0·0012 (3)	−0·0022 (3)	0·1441 (3)	2·6
O(3)	96	1	−0·0300 (3)	0·0770 (3)	0·0752 (3)	2·4
O(4)	96	1	−0·0740 (3)	0·0741 (3)	0·1774 (3)	2·1
Ca(II)	10·5	0·33 (3)	0·254 (2)	*x*	*x*	12·8
Ca(I′)	20·1	0·63 (1)	0·0692 (2)	*x*	*x*	1·5
Ca(III)	16·5	0·17 (1)	0·173 (1)	0·437 (1)	0·303 (1)	5·5
H_2O(1)	42·8	1·33 (5)	0·1681 (4)	*x*	*x*	6·0
H_2O(2)	8·5	0·53 (9)	0·	*x*	*x*	10·7
H_2O(3)	24·5	0·26 (3)	0·387 (3)	0·576 (2)	0·360 (2)	11·3
H_2O(4)	30·2	0·31 (3)	0·246 (2)	0·371 (2)	0·503 (2)	9·0
H_2O(5)	13·7	0·14 (2)	0·223 (2)	0·520 (2)	0·345 (2)	3·0
348 K						
Si	96	1	−0·0539 (2)	0·1238 (3)	0·0346 (2)	1·3
Al	96	1	−0·0553 (2)	0·0369 (2)	0·1216 (2)	1·1
O(1)	96	1	−0·1105 (6)	0·0022 (7)	0·1038 (6)	3·6
O(2)	96	1	−0·0035 (6)	−0·0038 (6)	0·1433 (5)	2·4
O(3)	96	1	−0·0339 (5)	0·0669 (6)	0·0622 (5)	1·9
O(4)	96	1	−0·0673 (6)	0·0784 (6)	0·1745 (6)	2·9
Ca(I)	10·9	0·68 (4)	0·	*x*	*x*	1·8
Ca(II)	11·9	0·37 (3)	0·242 (1)	*x*	*x*	4·1
Ca′(II)	5·3	0·16 (2)	0·223 (3)	*x*	*x*	1·6
Ca(I′)	8·7	0·27 (3)	0·072 (1)	*x*	*x*	2·7
Ca(III)	4·2	0·04 (1)	0·405 (6)	0·049 (6)	0·048 (6)	4·0
H_2O(1)	32·5	1·00 (9)	0·167 (1)	*x*	*x*	5·7
423 K						
Si	96	1	−0·0543 (2)	0·1232 (2)	0·0342 (2)	1·2
Al	96	1	−0·0562 (2)	0·0379 (2)	0·1216 (2)	1·3
O(1)	96	1	−0·1126 (6)	0·0016 (6)	0·1058 (6)	3·4
O(2)	96	1	−0·0032 (5)	−0·0033 (5)	0·1433 (5)	2·6
O(3)	96	1	−0·0355 (4)	0·0668 (4)	0·0604 (4)	1·8
O(4)	96	1	−0·0650 (5)	0·0793 (5)	0·1738 (6)	3·1
Ca(I)	14·2	0·88 (2)	0·	*x*	*x*	1·9
Ca(II)	20·4	0·64 (2)	0·2331 (4)	*x*	*x*	2·7
Ca(I′)	5·7	0·18 (2)	0·063 (2)	*x*	*x*	5·6
Ca(III)	5·4	0·06 (1)	0·399 (3)	0·093 (3)	0·090 (3)	3·1
H_2O(1)	10·9	0·34 (6)	0·164 (3)	*x*	*x*	6·2
573 K						
Si	96	1	−0·0539 (1)	0·1230 (1)	0·0336 (1)	1·1
Al	96	1	−0·0566 (1)	0·0369 (1)	0·1217 (1)	1·5
O(1)	96	1	−0·1122 (4)	0·0016 (4)	0·1063 (4)	2·9
O(2)	96	1	−0·0038 (4)	−0·0036 (4)	0·1411 (3)	2·3
O(3)	96	1	−0·0349 (4)	0·0670 (4)	0·0599 (4)	2·9
O(4)	96	1	−0·0612 (4)	0·0789 (4)	0·1736 (5)	3·4
Ca(I)	15·5	0·97 (2)	0·	*x*	*x*	2·0
Ca(II)	24·3	0·76 (2)	0·2256 (3)	*x*	*x*	3·0
Ca(I′)	2·8	0·09 (2)	0·058 (4)	*x*	*x*	3·2
Ca(III)	2·2	0·02 (1)	0·080 (6)	0·078 (6)	0·399 (6)	2·3
H_2O(1)	9·2	0·29 (6)	0·160 (4)	*x*	*x*	9·6
673 K						
Si	96	1	−0·0545 (2)	0·1230 (2)	0·0345 (2)	1·4
Al	96	1	−0·0560 (2)	0·0366 (2)	0·1216 (2)	1·0
O(1)	96	1	−0·1109 (5)	0·0007 (5)	0·1075 (5)	3·4
O(2)	96	1	−0·0040 (4)	−0·0031 (4)	0·1424 (4)	2·1
O(3)	96	1	−0·0354 (4)	0·0655 (4)	0·0636 (4)	1·8
O(4)	96	1	−0·0596 (5)	0·0785 (5)	0·1730 (5)	2·7
Ca(I)	14·6	0·91 (2)	0·	*x*	*x*	1·9
Ca(II)	29·0	0·91 (1)	0·2238 (2)	*x*	*x*	3·7
Ca(I′)	2·6	0·08 (2)	0·070 (7)	*x*	*x*	4·3
Ca(III)	2·7	0·03 (1)	0·122 (4)	−0·034 (4)	0·777 (4)	1·5
298 K (rehydrated)						
Si	96	1	−0·0529 (2)	0·1252 (3)	0·0365 (2)	1·6
Al	96	1	−0·0536 (2)	0·0367 (2)	0·1250 (3)	1·4
O(1)	96	1	−0·1041 (6)	−0·0005 (6)	0·1032 (6)	3·0
O(2)	96	1	−0·0017 (6)	−0·0028 (6)	0·1454 (5)	2·1
O(3)	96	1	−0·0332 (6)	−0·0781 (7)	0·0762 (6)	3·0
O(4)	96	1	−0·0723 (6)	0·0709 (7)	0·1805 (7)	2·9
Ca(II)	10·2	0·32 (2)	0·251 (1)	*x*	*x*	6·9
Ca(I′)	19·6	0·61 (2)	0·0687 (4)	*x*	*x*	2·2
Ca(III)	9·8	0·10 (1)	0·046 (2)	0·042 (2)	0·416 (2)	3·7
H_2O(1)	29·6	0·92 (5)	0·167 (1)	*x*	*x*	3·8
H_2O(2)	15·3	0·16 (3)	0·001 (3)	0·002 (3)	0·365 (3)	2·9
H_2O(3)	9·7	0·10 (3)	0·065 (4)	0·064 (4)	0·422 (4)	0·9
H_2O(4)	6·1	0·13 (4)	0·875	0·085 (5)	0·375	1·6

* Lists of observed and calculated structure factors and anisotropic thermal parameters have been deposited with the British Library Document Supply Centre as Supplementary Publication No. SUP 51458 (27 pp.). Copies may be obtained through The Executive Secretary, International Union of Crystallography, 5 Abbey Square, Chester CH1 2HU, England.

atomic distances (calculated from positional parameters) to non-framework atoms within 2–3·2 Å are listed in Table 3. In the Ca-exchanged form all Ca ions have been located, which is in marked contrast to hydrated Na*X* (Smolin, Shepelev, Butikova & Petranovsky, 1983).

The siting obtained for Ca cations in the hydrated zeolite is fairly consistent with Pluth & Smith (1973*b*), except for the interpretation of the electron density peak in site II. This peak was assigned by Pluth & Smith to water molecules because the distance to three framework O(2) atoms was too long (3·11 Å). In our case this distance is 2·75 Å and the investigation at different temperatures confirms the cation nature of this peak. An increase of temperature causes changes in the cation environments resulting in cation migration. In turn, the redistribution of cations in the crystal influences to some degree the geometry of the aluminosilicate framework. In Fig. 2 the siting of Ca cations and that of water molecules are compared for the six related structures of Ca-exchanged *X* zeolite: hydrated, dehydrated at 348, 423, 573, 673 K and rehydrated in air at 298 K. According to gravimetric analysis (Costenoble, Mortier & Uytterhoeven, 1978) at 348 K, approximately 60 water molecules remain in the unit cell. As 20 water molecules are sited in the β-cage, it may be assumed that the remaining molecules are accommodated in the supercages. They were not located. It can be seen that the water molecules in site II′ are the most strongly bonded. They are removed from the structure only on heating above 573 K.

The analysis of Fig. 2 clearly demonstrates that the dehydration at 348 K results in the migration of cations. The effect is most pronounced for sites I and I′: the population of the former being increased and that of the latter being reduced by approximately the same amount. The cation migration in the direction of hexagonal prisms is most probably due to the fact that after removal of water molecules the cations are in unsaturated coordination in the β-cages. In hexagonal prisms they find themselves in an octahedral oxygen environment. With a further increase of temperature up to 573 K the occupancy of site I increases and the number of Ca atoms in the β-cage decreases.

The population of cation position II also gradually increases with increasing degree of dehydration, depending on temperature. At the first stage some of the

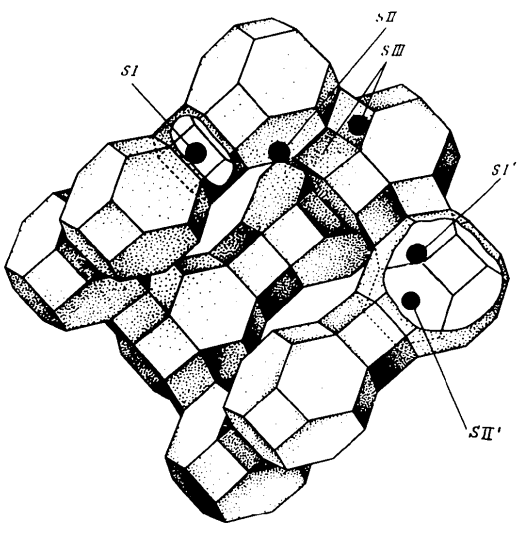

Fig. 1. The structure of *X* zeolites.

Table 3. *Interatomic distances* (<3·2 Å) *for the extra framework cation and* O *atoms*

298 K					
Ca(II)	–O(2)	2·75 (6)	$H_2O(1)$	–O(2)	3·02 (1)
	$-H_2O(4)$	3·14 (8)		$-H_2O(1)'$	3·06 (2)
Ca(I′)	–O(3)	2·50 (1)	$H_2O(2)$	–O(3)	2·80 (1)
	$-H_2O(1)$	2·52 (1)	$H_2O(3)$	–O(4)	3·10 (6)
	$-H_2O(2)$	3·00 (1)		–O(4)′	3·15 (6)
	–O(2)	3·14 (1)	$H_2O(4)$	–O(4)	2·83 (5)
Ca(III)	$-H_2O(4)$	2·24 (6)	$H_2O(5)$	–O(4)	2·70 (5)
	$-H_2O(3)$	2·40 (8)		$-H_2O(5)'$	2·78 (7)
	$-H_2O(3)'$	2·44 (7)			
	–O(4)	2·55 (2)			
	$-H_2O(5)$	2·59 (6)			
	$-H_2O(5)'$	2·63 (6)			
	$-H_2O(4)'$	2·74 (6)			
	–O(1)	2·97 (1)			
	$-H_2O(4)''$	3·01 (6)			
348 K					
Ca(I)	–O(3)	2·44 (1)	Ca(I′)	$-H_2O(1)$	2·40 (5)
	–Ca(I′)	3·13 (3)		–O(3)	2·67 (3)
Ca(II)	–O(2)	2·51 (3)	Ca(III)	–O(4)	2·4 (1)
	–O(4)	3·09 (3)		–O(1)	2·9 (1)
Ca′(II)	–O(2)	2·28 (7)		–Ca(III)′	2·9 (1)
	$-H_2O(1)$	2·45 (8)	$H_2O(1)$	$-H_2O(1)'$	2·96 (7)
	–O(4)	2·95 (7)		–O(2)	3·13 (4)
423 K					
Ca(I)	–O(3)	2·42 (1)	Ca(III)	–Ca(III)′	2·4 (1)
	–Ca(I)′	2·72 (5)		–O(1)	2·78 (7)
Ca(II)	–O(2)	2·34 (2)		–O(1)′	2·80 (7)
	–O(4)	2·98 (2)	$H_2O(1)$	$-H_2O(1)'$	2·8 (1)
	$-H_2O(1)$	3·01 (6)			
Ca(I′)	–O(3)	2·46 (5)			
	$-H_2O(1)$	2·67 (8)			
	–O(2)	3·10 (5)			
573 K					
Ca(I)	–O(3)	2·42 (1)	Ca(III)	–O(4)	2·2 (1)
	–Ca(I′)	2·54 (9)		–O(1)	2·7 (1)
Ca(II)	–O(2)	2·34 (1)		–O(1)′	2·7 (1)
	$-H_2O(1)$	2·85 (9)	$H_2O(1)$	$-H_2O(1)'$	2·5 (2)
	–O(4)	2·86 (1)			
Ca(I′)	–O(3)	2·35 (9)			
	$-H_2O(1)$	2·8 (1)			
	–O(2)	3·02 (9)			
673 K					
Ca(I)	–O(3)	2·45 (1)	Ca(I′)	–O(3)	2·6 (2)
	–Ca(I′)	3·0 (2)		–O(2)	3·2 (2)
Ca(II)	–O(2)	2·30 (1)	Ca(III)	–O(4)	2·29 (9)
	–O(4)	2·82 (1)		–O(1)	2·8 (1)
				–O(1)′	3·0 (1)
298 K (rehydrated)					
Ca(II)	–O(2)	2·65 (4)	$H_2O(1)$	$-H_2O(1)'$	3·00 (5)
	$-H_2O(2)$	2·85 (8)		–O(2)	3·06 (3)
	–O(4)	3·09 (4)	$H_2O(2)$	–O(4)	2·64 (7)
Ca(I′)	$-H_2O(1)$	2·52 (2)		$-H_2O(3)$	2·6 (1)
	–O(3)	2·57 (2)		$-H_2O(3)'$	3·1 (1)
	–O(2)	3·17 (2)		$-H_2O(3)''$	3·1 (1)
Ca(III)	–O(4)	2·52 (5)	$H_2O(3)$	–O(4)	2·5 (1)
	–Ca(III)′	2·63 (4)		–O(1)	3·1 (1)
	$-H_2O(3)$	2·8 (1)		–O(1)′	3·2 (1)
	$-H_2O(4)$	2·87 (4)	$H_2O(4)$	–O(4)	3·02 (9)
	$-H_2O(3)'$	3·0 (1)			
	–O(1)	3·14 (4)			

cations in this site may approach the O atoms of the framework by loosing water molecules from their environment. This could be the reason for the splitting of the electron density peak in site II. The increase in population of site II is most probably due to the migration of Ca atoms to this position from the neighbouring sites II′ and III. At 673 K, when practically all water molecules are removed, about 90% of all cations are sited in two positions, which is consistent with the data for dehydrated Ca*X* zeolite given by Pluth & Smith (1973*a*). The re-siting dynamics of the cations is shown in Fig. 3 as a function of temperature.

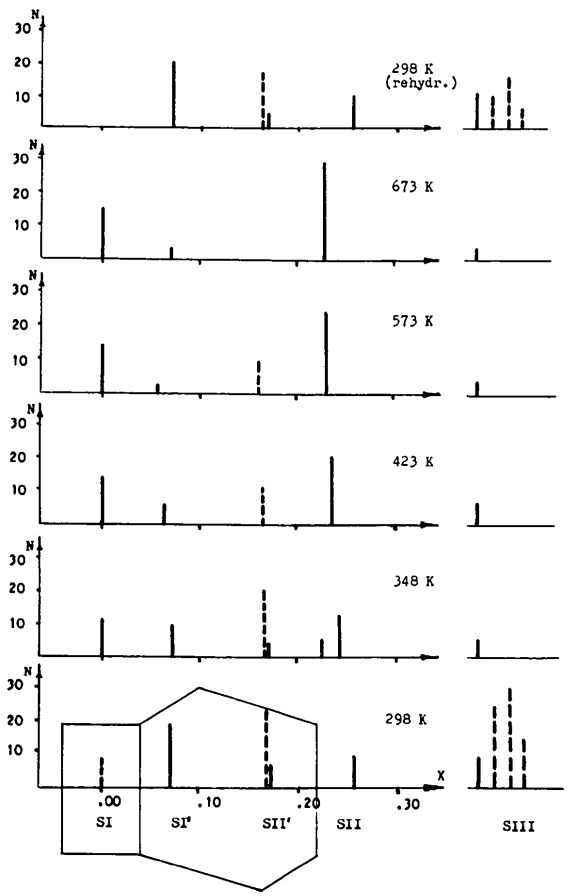

Fig. 2. Distribution of cations (full lines) and water molecules (dashed lines) in Ca*X* zeolite at various temperatures. *N* is the population of all sites.

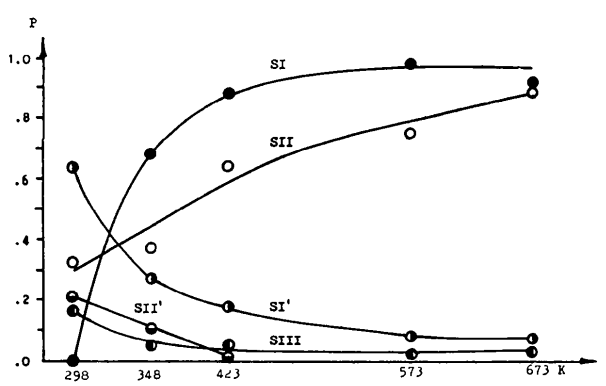

Fig. 3. The occupancy factors as a function of temperature in Ca*X* zeolite.

Table 4. *Selected* Si–O–Al *bond lengths* (Å) *and angles* (°) *for framework atoms*

	298 K	673 K		298 K	673 K
Si–O(1)	1·65 (1)	1·62 (1)	Al–O(1)	1·69 (1)	1·68 (1)
–O(2)	1·65 (1)	1·68 (1)	–O(2)	1·70 (1)	1·72 (1)
–O(3)	1·66 (1)	1·68 (1)	–O(3)	1·71 (1)	1·70 (1)
–O(4)	1·64 (1)	1·62 (1)	–O(4)	1·70 (1)	1·66 (1)
Average	1·65	1·65	Average	1·70	1·69

	298 K	348 K	423 K	573 K	673 K	298 K (rehydrated)
Si–O(1)–Al	139·8 (5)	132·6 (9)	128·2 (9)	127·8 (6)	128·0 (8)	143·9 (9)
Si–O(2)–Al	143·0 (5)	141·8 (9)	139·7 (8)	144·0 (6)	142·2 (7)	141·8 (9)
Si–O(3)–Al	137·9 (5)	129·0 (8)	128·2 (7)	128·4 (6)	130·3 (7)	143·2 (9)
Si–O(4)–Al	139·1 (5)	155·2 (9)	160·1 (9)	165·9 (8)	167·8 (9)	137·7 (9)
Average	140·0	139·6	139·0	141·5	142·1	141·6

During rehydration an inverse cation migration takes place and the site occupancies become close to those for the initial hydrated form. However, the new distribution of water molecules is slightly different. For example, after rehydration the water molecules did not return to the hexagonal prism. This fact is probably due to cation blocking of the prism windows.

The changes in cation siting during dehydration cause marked variations in the Si–O–Al angles. The Si–O and Al–O bond distances in SiO_4 and AlO_4 tetrahedra are not so sensitive, and therefore in Table 4 these values are given for the two extreme temperatures only. The values of the Si–O–Al angles are given for all temperatures. Despite the fact that some angles change significantly, their mean values at various temperatures are similar, which could explain the constancy in the unit-cell size.

References

ANDRIANOV, V. I., SAPHINA, Z. I. & TARNOPOLSKY, B. L. (1974). *J. Struct. Chem.* **15**, 911–917.

BENNET, J. M. & SMITH, J. V. (1968*a*). *Mater. Res. Bull.* **3**, 633–642.

BENNET, J. M. & SMITH, J. V. (1968*b*). *Mater. Res. Bull.* **3**, 933–940.

BOGOMOLOV, V. N. & PETRANOVSKY, V. P. (1986). *Zeolites*, **6**, 418–419.

COSTENOBLE, M. L., MORTIER, W. J. & UYTTERHOEVEN, J. B. (1978). *J. Chem. Soc. Faraday Trans.* 1, **2**, 466–476.

CRUICKSHANK, D. W. J. (1965). *Computing Methods in Crystallography*, edited by J. S. ROLLET, pp. 112–116. New York: Pergamon Press.

HANSON, H. P., HERMAN, F., LEA, J. D. & SKILLMAN, S. (1964). *Acta Cryst.* **17**, 1041–1044.

OATLEY, S. & FRENCH, S. (1982). *Acta Cryst.* A**38**, 537–549.

PLUTH, J. J. & SMITH, J. V. (1973*a*). *Mater. Res. Bull.* **7**, 1311–1322.

PLUTH, J. J. & SMITH, J. V. (1973*b*). *Mater. Res. Bull.* **8**, 459–468.

SMOLIN, YU. I., SHEPELEV, YU. F., BUTIKOVA, I. K. & PETRANOVSKY, V. P. (1983). *Kristallografiya*, **28**, 72–78.